01 Feb 2009

Power Sharing in a Double-Input Buckboost Converter using Offset Time Control

Deepak Somayajula

Mehdi Ferdowsi
Missouri University of Science and Technology, ferdowsi@mst.edu

Recommended Citation

D. Somayajula and M. Ferdowsi, "Power Sharing in a Double-Input Buckboost Converter using Offset Time Control," *Proceedings of the 24th Annual IEEE Applied Power Electronics Conference and Exposition (2009, Washington, D.C.)*, pp. 1091-1096, Institute of Electrical and Electronics Engineers (IEEE), Feb 2009.
The definitive version is available at https://doi.org/10.1109/APEC.2009.4802799

Power Sharing in a Double-Input Buckboost Converter Using Offset Time Control

Deepak Somayajula, *Student Member*, *IEEE* and Mehdi Ferdowsi, *Member*, *IEEE*
Missouri University of Science and Technology
Email: dbsv2b@mst.edu and ferdowsi@mst.edu

***Abstract*—Multi-input power electronic converters have been gaining popularity in applications such as renewable energy sources and hybrid electric vehicles due to their reduced component count. In this paper, a new control method is introduced and successfully applied to a double-input buckboost converter to adjust the power supplied by each one of the sources. The control scheme is based on controlling the offset time between the switching commands while switching frequency is kept constant. Theoretically, it is proved that the offset time between the switch commands has a direct impact on the amount of current drawn from each source. The proposed control method has a very fast dynamic response and improves the stability of traditional controllers. Simulation results agree with the theoretical analysis.**

***Index terms*—Double-input buckboost converter; Offset time control; Power sharing**

I. INTRODUCTION

Renewable energy sources have become more popular due to their environmentally friendliness. Energy sources such as wind and solar are intermittent and unpredictable; therefore, they are not highly reliable. In order to address this issue, renewable sources are either combined with each other or with an energy storage system to form a hybrid energy system. Batteries, ultracapacitors, and flywheels are the most common energy storage mechanisms used to hybridize energy systems. Hybrid electric powertrain are another example for energy systems with multiple sources. Hybridization can also be accomplished at the energy storage level to combine ultracapacitors and batteries together in order to get a high power density and high energy density storage system. In all these applications, a dc-dc converter is traditionally used to interface each energy related component with the rest of the system. Utilizing several dc-dc converters is expensive, bulky, less efficient, and hard to control. Replacing several converters with a single isolated or non-isolated multi-input converter has been reported in the literature [1-16]. Among several advantages [7], reduced component count and simplicity in control make multi-input converters attractive options to be utilized in hybrid energy systems which are comprised of more than one energy source.

Several non-isolated double-input dc-dc converters have been introduced, analyzed, and compared in the literature [9-16] including double-input buck, buckboost, and buck-buckboost converters [9]. Different approaches to synthesize double-input converters have also been reported earlier [13-19]. Most of the work reported in this field only covers topology exploration and steady state operation of such converters; though in some papers, the control aspects for specific multi-input topologies are discussed [20-23]. Control of the amount of power drawn from each of the sources in a hybrid energy system is important. When the power supplied by one of the sources decreases, the power supplied by other sources must be managed effectively to meet the load demand. Power sharing is necessary in hybrid energy systems like the wind-solar or battery-ultracapacitor combinations. For instance, on a cloudy day when the amount of solar power being supplied is low, the amount of power from other energy sources needs to increase. Also, in a battery-ultracapacitor combination when the ultracapacitor is discharged, the power drawn from the battery should be increased to meet the load demand. Thus the controller must be able to control the amount of power flowing out from different sources.

In [9], the importance of battery and ultracapacitor combination for hybrid electric vehicles is emphasized and the double-input buckboost converter topology is presented. In this paper, the control of a double-input buckboost converter (see Fig. 1) is discussed. Power sharing between the sources (battery and ultracapacitor) is analyzed for a variable load where the battery is supplying constant power and the ultracapacitor has to meet the excess load demand. It is proven that the offset time between the switch commands has a direct impact on the power sharing of the two sources. The proposed control method is called offset time control. A brief introduction of the double-input buckboost converter is presented in section II. Section III presents the offset time control scheme and the equations that govern the control scheme. In section IV, the physical model to realize the control scheme is presented. Simulation results are presented in sections V, VI, and VII. Section VIII has the conclusions.

II. DOUBLE-INPUT BUCKBOOST CONVERTER

A double-input buckboost converter is shown in Fig. 1 [9, 12, 16, and 21]. Switch S_1 can be any kind of switch as long as V_1 is greater than V_2. However, if V_1 is not guaranteed to be greater than V_2 then S_1 needs to be a reverse-blocking switch, such as an IGBT [13]. The double-input buckboost converter

978-1-422-2812-0/09/$25.00 ©2009 IEEE

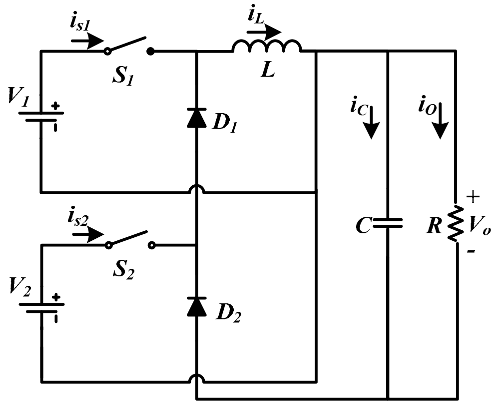

Fig. 1. Double-input buckboost converter

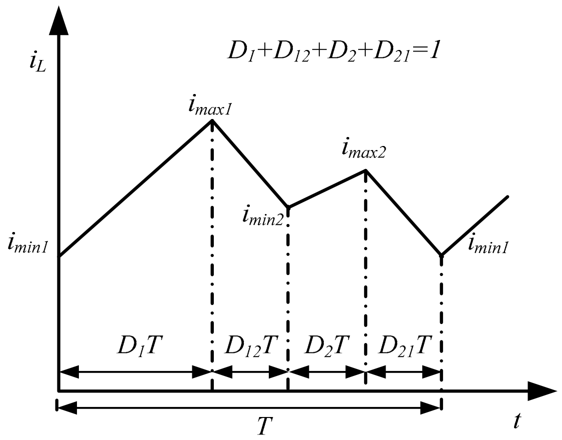

Fig. 2. Inductor current waveform

has mode restriction and it cannot be powered by both sources at the same time. In other words, both switches S_1 and S_2 cannot be ON at the same time [9]. In Fig. 2, a typical inductor current waveform for the converter is shown where D_1 and D_2 are the ON time duty ratios and D_{12} and D_{21} are the offset time duty ratios of switches S_1 and S_2, respectively.

Steady-state output voltage V_{out} of the converter [9, 14] can be described as

$$V_{out} = \frac{D_1 V_1}{(1 - D_1 - D_2)} + \frac{D_2 V_2}{(1 - D_1 - D_2)} \tag{1}$$

Average inductor current I_L for a resistive load R [12] is

$$I_L = < i_L > = \frac{V_O}{R(1 - D_1 - D_2)} \tag{2}$$

The ratio of switch currents i_{s1} to i_{s2} is

$$\frac{< i_{s1} >}{< i_{s2} >} = \alpha \tag{3}$$

III. OFFSET TIME CONTROL SCHEME

Alpha (α) is proportional to the ratio of power drawn from the sources V_1 and V_2. The amount of power drawn from each source can thus be varied by varying α which can be varied by varying the offset time which is time delay $D_{12}T$ between the switches S_1 and S_2 in Fig. 2. i_{min1} can be related to i_{max1} from Fig. 2 as

$$i_{\min 1} = i_{\max 1} - \frac{V_1}{L} D_1 T \tag{4}$$

Similarly, i_{min2} can be obtained from i_{max1} as

$$i_{\min 2} = i_{\max 1} - \frac{V_{out}}{L} D_{12} T \tag{5}$$

And i_{max2} is related to i_{min2} by the following equation

$$i_{\max 2} = i_{\min 2} + \frac{V_2}{L} D_2 T \tag{6}$$

The average switch currents $<i_{s1}>$ and $<i_{s2}>$ are given by the following equations as:

$$< i_{s1} > = (i_{\max 1} + i_{\min 1}) \frac{D_1}{2} \tag{7}$$

$$< i_{s2} > = (i_{\max 2} + i_{\min 2}) \frac{D_2}{2} \tag{8}$$

From (5) and (6), it can be seen that inductor current values i_{max1} and i_{max2} are related to each other. From (5), it can be seen that i_{min2} is dependent on the offset time $D_{12}T$. And from (8), it can be observed that the average value of the current supplied by V_2 i.e. i_{s2} is dependent on i_{max2} and i_{min2} which are both in turn dependent on $D_{12}T$. Therefore it can be concluded that by varying offset time $D_{12}T$ the average value of switch current i_{s2} can be varied while maintaining all other parameters constant. Thus the value of α can be controlled by varying $D_{12}T$. By substituting (7) and (8) into (3) and by eliminating i_{min1}, i_{max2}, and i_{min2} using (4), (5), and (6) the following equations can be obtained.

$$i_{\max 1} = \frac{\frac{1}{2Lf}[2V_0 D_2 D_{12} - V_2 D_2^2 - \frac{V_1 D_1^2}{\alpha}]}{(D_2 - \frac{D_1}{\alpha})} \tag{9}$$

$$\begin{aligned} < i_L > = i_{\max 1} - \frac{1}{2Lf}[D_1 V_1 - D_2 V_2 + D_1 D_2 (V_2 - V_1) \\ + 2D_2 (V_2 + V_0) D_{12}] \end{aligned} \tag{10}$$

In (9), a relation for i_{max1} in terms of α and D_{12} is obtained; however, i_{max1} needs to be eliminated to find a relationship between D_{12} and α. This relationship can be obtained by combining (2), (9), and (10) to eliminate i_{max1}. Thus, it can be shown that the ratio of power drawn from each of the sources can be controlled by varying the offset time duty ratio D_{12} of the converter. A typical plot between α and D_{12} is shown in Fig. 3 where α_{min} and α_{max} give the range in which α can vary for given operating points of the converter which is determined by the value of D_1 (D_2 depends on D_1 in order to have a constant output voltage). As it can be observed from Fig. 3, the relationship between α and D_{12} is almost linear.

In this paper it is assumed that switch S_1 is turned ON at the beginning of the switching cycle and D_{12} is determined by the

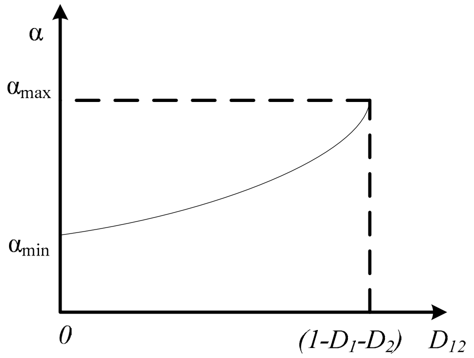

Fig. 3. Typical plot for α vs. D_{12}

controller. Similar analysis can be presented if switch S_2 is turned ON at the beginning of the cycle. In the latter case D_{21} will be the control parameter.

IV. CONTROL SCHEME REALIZATION

Power sharing in a double-input buckboost converter is carried out in two stages as shown in Fig. 4. In the first stage the outer loop is regulated by the system level controller for load regulation and in the second stage the inner loop is regulated by the power sharing controller to obtain the desired power sharing between the two sources. The control objective of the power sharing controller is to supply constant power from battery and to meet the excess load demand by ultracapacitor. The power sharing controller shown in Fig. 5 can be realized by comparing the real value of α which is obtained at the end of each switching cycle to α_{ref} and integrating the error to obtain the offset time duty ratio D_{12} between the switch commands. α_{ref} can be replaced with proportional switch currents I_{ref1} or I_{ref2} where I_{ref1} and I_{ref2} are the average switch current values of switches S_1 and S_2 respectively. The offset time control can be carried out by programming either I_{ref1} or I_{ref2} externally. In the former case, controlling D_{12} leads to instability so D_{21} should be the control parameter whereas in the latter case controlling D_{21} leads to instability and D_{12} should be the control parameter. The outer loop system level controller should maintain a constant output voltage and should be able to determine the duty ratios D_1 and D_2. The system level controller has to decide upon an energy management strategy based on various factors like the battery state of charge (SOC), the ultracapacitor SOC, and load demand. The system level controller has to then decide on a proper value of I_{ref1} or I_{ref2} depending on the choice of the control parameter which is either D_{21} or D_{12}. Based on the inputs given to the power sharing controller, it has to decide on the value of D_{12} in order to meet the control objective of maintaining output voltage regulation while sharing the power between the two sources based on the load demand and ultracapacitor SOC. The PWM block has the following inputs D_1, D_2, and D_{12} and it has to generate the control pulses for switches S_1 and S_2, respectively. The control pulses for S_2 can be generated as shown in Fig. 6 by using the sawtooth ramps *sawtooth1* and *sawtooth2* and the control voltages $V_c\_S_{12}$ and $V_c\_S_2$ which are control voltages proportional to D_{12} and D_2, respectively.

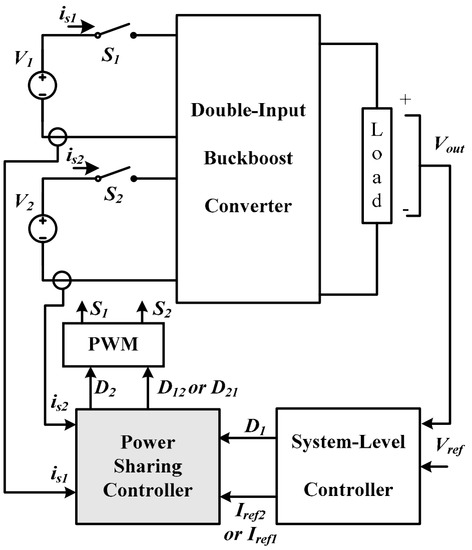

Fig. 4. Block diagram of the overall system

Power Sharing Controller

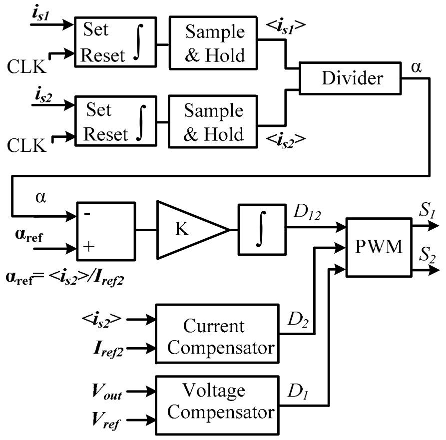

Fig. 5. Block diagram of power sharing controller

V. SIMULATION RESULTS FOR OPEN-LOOP RESPONSE

The double-input buckboost converter with inner loop programmable power sharing controller was modeled in MATLAB Simulink. The overall system was simulated for the following parameters $V_1 = 40$V (ultracapacitor), $V_2 = 70$V (battery), $V_{out} = 90$ V, $f_s = 50$ kHz, $L = 50$ μH for continuous conduction mode, and $C = 100$ μF. Initially the relationship between α and D_{12} is plotted for 3 different values of D_1 (0.4, 0.3, 0.2). D_2 values are dependent on D_1 if it is assumed that the output voltage remains constant at 90V. D_2 values can be found by substituting all other parameters in the steady state voltage transfer ratio (1). From Fig. 7, it can be concluded that α can be varied by varying D_{12} when D_1 and D_2 are kept constant and the range in which α can be varied depends on D_1 and D_2. Also from Fig. 7, it can be observed that α increases almost linearly proportional with D_{12}. Therefore, it is easier to increase average current $<i_{s1}>$ supplied from the ultracapacitor when average current $<i_{s2}>$ supplied from the battery is constant by increasing D_{12}.

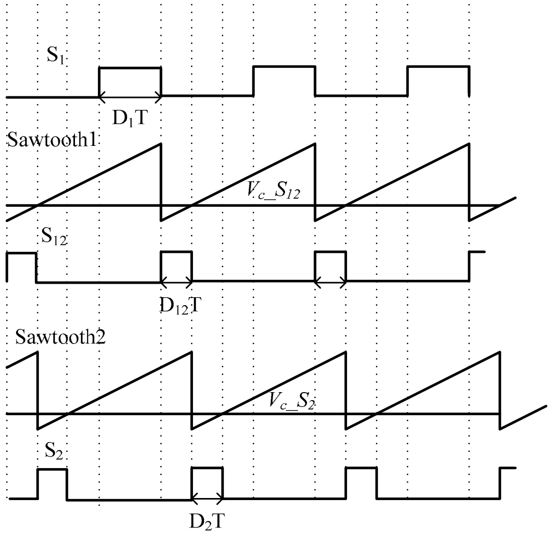

Fig. 6. Pulse width modulation block and delay D_{12} between S_1 and S_2

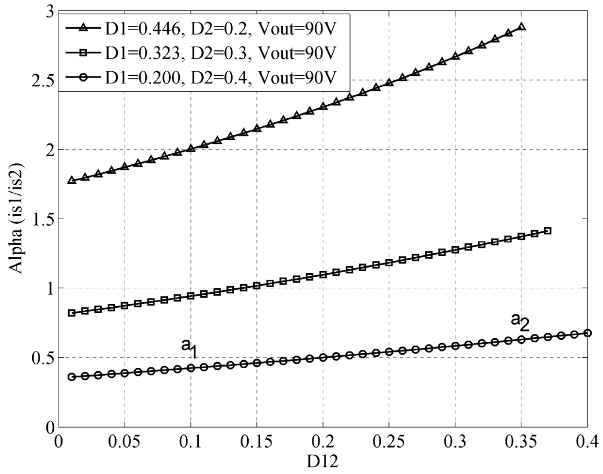

Fig. 7. Variations of α vs. D_{12}

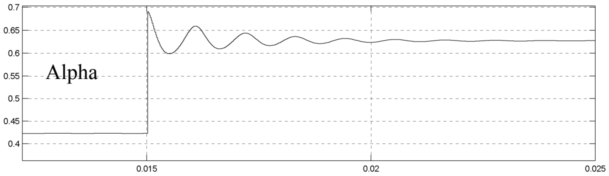

Fig. 8. Open-loop step response of α for a step change in D_{12} from 0.1 to 0.35

The system is then simulated to obtain an open-loop step response for α. A step change in D_{12} from 0.10 to 0.35 occurs at t=0.015 s when D_1 and D_2 are kept constant at 0.2 and 0.4, respectively. In this case, both the inner loop power sharing controller and the outer loop system level controller are open. The value of α is expected to change from 0.4235 to 0.6289 (points a_1 and a_2, respectively) as predicted from the plot in Fig. 7. The step response is shown in Fig. 8 which indicates a very fast dynamic. The value of α changes almost instantaneously. This indicates that the inner loop dynamics is of zero order.

VI. SIMULATION RESULTS FOR ONE-OUTER LOOP CLOSED

The double-input buckboost converter can be controlled to have output voltage regulation and constant battery current with the three control parameters D_1, D_2, and D_{12}. The control objective can be achieved by controlling 2 of the 3 control parameters. Compensators are designed to control the 3 control parameters. They consist of an inner loop compensator which regulates the offset time $D_{12}T$ and is an integrator (40,000/s) and 2 outer loop compensators which include a voltage compensator (0.01+50/s) to generate duty ratio D_1 and a current compensator (0.01+1,500/s) to generate duty ratio D_2. Converter can be controlled by controlling 2 of these 3 control parameters. In this section, simulation results will be presented for cases where 2 of the 3 control parameters are controlled i.e. for cases with one outer loop closed and the inner loop closed. Two such cases exist, 1) D_1 and D_{12} are controlled and 2) D_2 and D_{12} are controlled. In both cases, the output voltage is desired to remain constant at 90 V and the average battery current $<i_{s2}>$ has to remain constant at 9 A for a step change in load from 8 to 10 Ω. Figs. 9 and 10 have the average current of both the sources and the output voltage waveforms for cases 1 and 2, respectively. As can be seen from Fig. 9, for the case where only D_1 and D_{12} are controlled with D_2 constant at 0.4 then the control objective of maintaining the output voltage and average battery current constant at 90 V and 9 A, respectively is met. However, bigger step changes in load tend to cause oscillations in the output voltage and the input currents. From Fig. 10 it can be concluded that when D_2 and D_{12} are controlled the output voltage settles at a suboptimal value of 80 V initially and reaches the steady state value of 90 V only after the step change in load and the average battery current stays constant at 9 A even in this case. Thus it can be concluded with only outer loop variable D_1 or D_2 controlled the control objective is not effectively met. And therefore simulation results are presented in section VII where the both the outer loop variables D_1 and D_2 are controlled.

VII. SIMULATION RESULTS FOR CLOSED-LOOP RESPONSE

Closed-loop response of the system can be obtained when both the outer loops are closed. The same sets of compensators are used for controlling D_1, D_2, and D_{12}. For the sake of comparison, the results are obtained for two cases 1) without offset time control i.e. D_1 and D_2 are controlled and 2) with offset time control i.e. D_1, D_2, and D_{12} are controlled. In both cases, a step change in load is assumed from 3 to 10 Ω and average current $<i_{s2}>$ from battery is expected to remain constant at 9 A even after the step change takes place at t=0.015 s. The output voltage remains constant at 90V for both the cases. Figs. 11 and 12 show the average current waveforms of both the sources for cases 1 and 2, respectively. It can be clearly observed from Fig. 11 that the results for the step change in load are better for case 2 in which offset time control is implemented. The control objectives of keeping the

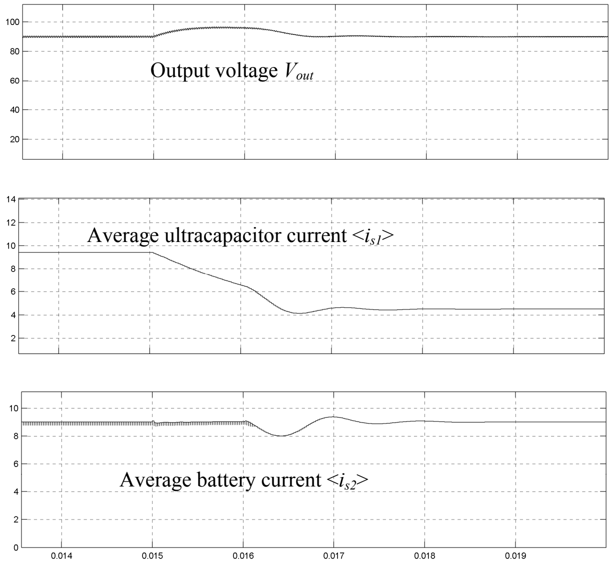

Fig. 9. Output voltage and Average current waveforms for both sources for a step change in load from 8 to 10 Ω **with D_1 and D_{12} controlled**

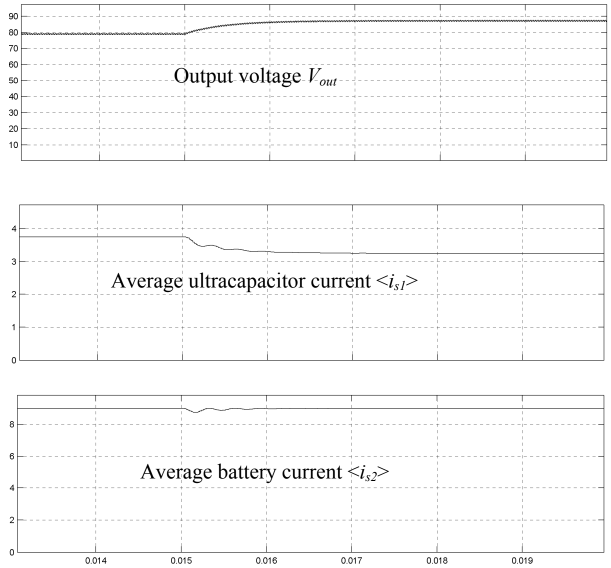

Fig. 10. Output voltage and Average current waveforms for both sources for a step change in load from 8 to 10 Ω **with D_2, and D_{12} controlled**
Average ultracapacitor current $<i_{s1}>$

output voltage and average battery current $<i_{s2}>$ constant and meeting the excess load demand from the ultracapacitor have been achieved in both the cases. However, the system is oscillatory when there is no offset time control as can be seen in Fig. 12. This clearly indicates the need for the offset time control algorithm in the double-input buckboost converter.

VIII.CONCLUSIONS

Offset time control scheme was introduced and applied to a double-input buckboost converter. It was theoreticaly proved that adjusting the offsett time between the switch commands has a direct impact on the current drawn from each source.

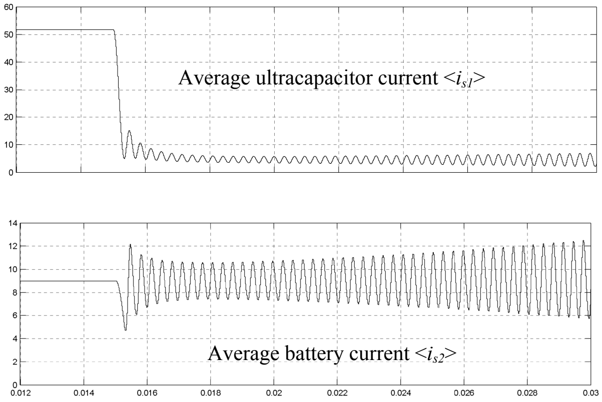

Fig. 11. Average current waveforms for both sources for a step change in load from 3 to 10 Ω **without** offset time control

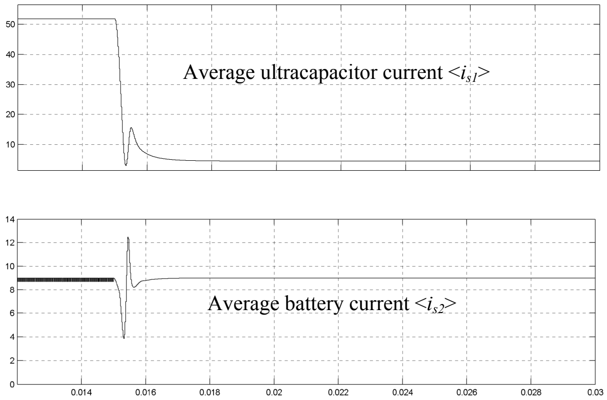

Fig. 12. Average current waveforms for both sources for a step change in load from 3 to 10 Ω **with** offset time control

Simulation results show that offset time control has a zero-order dynamics. This control method was used for the integration of batteries and ultracapacitors in a hybrid vehicle where the battery unlike the ultracapacitors is expected to supply a constant current against the variations of the load. It is shown that the control objective can be achieved using simple PI controllers as current and the voltage compensators. The results show that applying offset time control improves the stability and dynamic performance of the system while the control objectives are better achieved. Extensive compensator design based on the transfer functions obtained through small signal analysis for both the inner and the outer loops is left for future work.

REFERENCES

[1] R. M. Schupbach, J. C. Balda, M. Zolot, and B. Kramer, "Design methodology of a combined battery-ultracapacitor energy storage unit for vehicle power management," in *Proc. IEEE Power Electronics Conf.,* 15-19 Jun. 2003, vol. 1, pp. 88-93.

[2] L. Solero, F. Caricchi, F. Crescimbini, O. Honorati, and F. Mezzetti, "Performance of a 10 kW power electronic interface for combined wind/PV isolated generating systems," in *Proc. IEEE Power Electronics Specialists Conf. (PESC),* Jun. 1996, vol. 2, pp. 1027–1032.

[3] A. D. Napoli, F. Crescimbini, S. Rodo, and L. Solero, "Multiple input dc-dc power converter for fuel-cell powered hybrid vehicles", in *Proc.*

IEEE Power Electronics Specialists Conf. (PESC), Jun. 2002, vol. 4, pp. 1685–1690.

[4] H. Li, Z. Du, K. Wang, L. M. Tolbert, and D. Liu, "A hybrid energy system using cascaded H-bridge converter," in *Proc. IEEE Industrial Applications Conf.,* vol. 1, Oct. 2006, pp.198-203.

[5] Y. M. Chen, Y. C. Liu, and F. Y. Wu, "Multi-input converter with power factor correction, maximum power point tracking, and ripple-free input currents," *IEEE Trans. Power Electronics,* vol. 19, pp. 631-639, May 2004.

[6] Y. M. Chen, Y. C. Liu, F. Y. Wu, and Y. E. Wu, "Multi-input converter with power factor correction and maximum power point tracking features," in *Proc. IEEE Applied Power Electronics Conf. and Exposition (APEC),* vol. 1, Mar. 2002, pp. 490-496.

[7] H. Tao, A. Kotsopoulos, J. L. Duarte, and M. A. M. Hendrix, "Family of multiport bidirectional dc-dc converters," in *Proc. IEEE Electric Power Applications,* vol. 153, May 2006, pp. 451 - 458.

[8] H. Tao, A. Kotsopoulos, J. L. Duarte, and M. A. M. Hendrix, "Triple-half-bridge bidirectional converter controlled by phase shift and PWM", in *Proc. IEEE Applied Power Electronics Conf. and Exposition (APEC), Dallas, TX,* USA, Mar. 2006,.pp. 1256-1262.

[9] K. P. Yalamanchili, M. Ferdowsi, and K. Corzine, "New double input dc-dc converter for automotive applications", in *Proc. IEEE Vehicle Power and Propulsion Conf.,* 6-8 Sept. 2006, pp. 1-6.

[10] K. P. Yalamanchili and M. Ferdowsi, "Review of multiple input DC-DC converters for electric and hybrid vehicles," in *Proc. IEEE Vehicle Power and Propulsion Conf.,* 7-9 Sept. 2005, pp. 160-163.

[11] Y. M. Chen and Y. C. Liu, "Development of multi-port converters for hybrid wind-photovoltaic power system," in *Proc. IEEE Region 10 International Conf. on Electrical and Electronic Technology,* vol.2, Aug. 2001, pp. 804-808.

[12] K. P. Yalamanchili, "Multi-input dc-dc converters for combined energy storage systems in hybrid electric vehicles," *M. S. Thesis, University of Missouri-Rolla,* Dec. 2006.

[13] K. Gummi, "Derivation of new double-input dc-dc converters using Building Block Methodology," *M. S. Thesis, University of Missouri-Rolla,* Dec. 2007.

[14] K. Gummi and M. Ferdowsi, "Synthesis of double-input dc-dc converters using single pole triple throw switch as a building block," in *Proc. IEEE Power Electronics Specialists Conf. (PESC), Greece,* Jun. 2008.

[15] K. Gummi and M. Ferdowsi, "Derivation of new double-input converters using H-Bridge cells as Building Blocks," *to appear in Proc. IEEE Industrial Electronics Conf., Orlando, FL, USA,* November 2008.

[16] B. G. Dobbs and P. L. Chapman, "A multiple-input dc-dc converter topology," *IEEE Power Electronics Letters,* vol. 1, pp. 6-9, Mar. 2003.

[17] Y. M. Chen, Y. C. Liu, and F. Y. Wu, "Multi-input DC/DC converter based on the multiwinding transformer for renewable energy applications," *IEEE Trans. Industry Applications.,* vol.38, pp. 1096-1104, Aug. 2002.

[18] N. D. Benavides and P. L. Chapman, "Object-oriented modeling of a multiple-input multiple-output flyback converter in Dymola*,"* in *Proc. IEEE workshop on Computer Power Electronics,* 15-18 Aug. 2004, pp. 150-160.

[19] Y. C. Liu and Y. M. Chen, "A systematic approach to synthesizing multi-input dc/dc converters," in *Proc. IEEE Power Electronics Specialists Conf. (PESC),* Jun. 2007, pp. 2626-2632.

[20] Y. M. Chen, Y. C. Liu, and S. H. Lin, "Double-input pwm DC/DC converter for high/low-voltage sources," *IEEE Trans. Industrial Electronics,* vol. 53, pp. 1538-1545, Oct. 2006.

[21] N. D. Benavides and P. L. Chapman, "Power budgeting of a multiple-input buck-boost converter*," IEEE Trans. Power Electronics,* vol. 20, pp. 1303-1309, Nov. 2005.

[22] Y. M. Chen, Y. C. Liu, S. C. Hung, and C. S. Cheng, "Multi-input inverter for grid-connected hybrid pv/wind power system," in *Proc. IEEE Trans. Power Electronics,* vol. 22, pp. 1070-1077, May 2007.

[23] Y. M. Chen, C. S. Cheng, and H. C. Wu, "Grid-connected hybrid PV/wind power generation system with improved DC bus voltage regulation strategy," in *Proc. IEEE Applied Power Electronics Conf. (APEC),* Mar. 2006, pp. 1088-1094.